Electronic Supplementary Material (ESI) for Polymer Chemistry

Supplementary Information

Determining the Mark-Houwink Parameters of Nitrile Rubber: A Chromatographic Investigation of the NBR Microstructure

Christoph J. Dürr,[†] *Lebohang Hlalele,*[†] *Maria Schneider-Baumann,*[†] *Andreas Kaiser,*[‡] *Sven Brandau*[‡] *and Christopher Barner-Kowollik**[†].

[†]Preparative Macromolecular Chemistry, Institut für Technische Chemie und Polymerchemie, Karlsruhe Institute of Technology (KIT), Engesserstr. 18, 76128 Karlsruhe and Institut für Biologische Grenzflächen, Karlsruhe Institute of Technology (KIT), Hermann-von-Helmholtz Platz1, 76344 Eggenstein-Leopoldshafen, Germany

[‡]Lanxess Emulsion Rubber, BP 7 – Z.I. Rue du Ried, 67610 La Wantzenau, France.

Table S1. Experimental details and analytical data of NBR samples investigated in the study. In the manuscript the samples are referred to by quoting the polymerization run and the time samples were taken during polymerization, *e.g.* A_{15} for the first entry.[a]

run	*t* (h)	*p*[b] (%)	M_n[c] (kg·mol^{-1})	M_m[c] (kg·mol^{-1})	*Đ*[c]		$[\eta]$[d] (ml·g^{-1})	M_{LS}[e] (kg·mol^{-1})
A	15	4.5	122	197	1.6	**a**	146.1	103.5
						b	154.8	103.0
						c	146.0	101.0
A	16	4.9	120	189	1.7	**a**	145.1	104.8
						b	142.5	104.9
						c	144.2	103.3
A	20	6.6	111	187	1.7	**a**	139.6	101.9
						b	138.7	102.1
						c	137.1	102.2
A	22	7.4	110	184	1.7	**a**	138.2	97.7
						b	139.8	97.2
						c	136.7	96.5
B	3	1.5	120	204	1.7	**a**	149.1	102.6
						b	150.3	111.4
						c	149.8	108.9
B	6	3.4	118	203	1.7	**a**	154.4	105.5
						b	154.0	106.8
						c	153.5	108.4
B	8	4.8	122	199	1.6	**a**	143.9	102.2
						b	142.9	101.4
						c	144.8	102.5
B	22	12.7	94	176	1.9	**a**	147.7	108.2
						b	147.3	105.6
						c	148.3	106.6

C	5	4.8	116	198	1.7	**a**	146.4	100.1
						b	144.7	104.7
						c	145.9	102.1
C	8	8.9	113	188	1.7	**a**	142.0	103.7
						b	141.2	104.0
						c	136.8	136.8
C	22	21.6	90	173	1.9	**a**	126.5	97.8
						b	123.8	96.4
						c	124.4	97.5
C	24	23.1	84	170	2.0	**a**	125.0	99.9
						b	125.6	96.3
						c	125.8	96.8
D	3	4.6	93	156	1.7	**a**	126.6	78.7
						b	126.7	79.7
						c	126.8	79.6
D	5	9.1	86	145	1.7	**a**	119.8	77.5
						b	122.5	78.1
						c	121.0	78.3
D	7	11.7	91	150	1.7	**a**	117.8	77.3
						b	116.2	78.4
						c	118.3	80.0
D	8	13.0	85	148	1.7	**a**	113.7	80.0
						b	119.4	78.2
						c	115.1	79.6
D	22	28.5	85	156	1.8	**a**	112.6	81.2
						b	112.6	80.5
						c	114.6	80.5
D	24	30	85	157	1.8	**a**	111.6	86.9
						b	111.2	86.5
						c	110.8	90.9
E	1.33	1.7	73	120	1.6	**a**	102.0	62.2
						b	102.6	61.7
						c	103.8	61.7

E	2	3.1	73	116	1.6	**a**	100.7	59.9
						b	99.1	59.4
						c	99.86	59.9
E	2.66	4.5	68	112	1.6	**a**	96.2	60.1
						b	95.0	59.5
						c[f]	96.5	59.0
E	3	4.9	70	113	1.6	**a**	95.8	59.2
						b	95.9	58.7
						c	95.7	59.7
F	1	2.7	81	126	1.6	**a**	105.7	65.1
						b	104.8	66.3
						c	105.0	66.3
F	1.66	4.9	74	116	1.6	**a**	98.0	60.4
						b	97.0	60.3
						c	97.2	60.4
F	2.66	8.5	71	113	1.6	**a**	93.1	57.1
						b	94.8	57.1
						c	95.9	57.7
F	3.33	11.2	74	112	1.5	**a**	94.2	57.9
						b	96.0	58.7
						c	94.9	58.4
G	17	1.9	40	64	1.6	**a**	69.6	32.0
						b	67.0	32.2
						c	66.6	32.0
G	20	2.6	44	71	1.6	**a**[f]	68.6	36.5
						b	71.0	36.7
						c	71.6	37.2
G	22	3.2	46	78	1.7	**a**	74.9	39.6
						b	77.2	39.0
						c	76.8	39.1
H	4	4.5	24	36	1.5	**a**	41.0	16.8
						b	38.6	16.9
						c	39.6	17.2

H	6	6.8	33	49	1.5	**a**	52.3	23.6
						b	52.7	23.3
						c	50.4	23.0
H	7	8.7	36	54	1.5	**a**	52.1	26.7
						b	53.0	26.9
						c	51.8	27.1
H	8	10.5	40	60	1.5	**a**	58.9	28.4
						b	58.9	30.5
						c	59.5	30.1
H	22	28.7	65	114	1.7	**a**	92.9	62.4
						b	90.3	62.8
						c	93.1	63.0
H	24	29.3	73	123	1.7	**a**	97.7	66.8
						b	96.0	66.1
						c	98.3	66.6

[a] Experimental details of the polymerizations are provided in Table 1 in the main manuscript. [b] Conversion was determined gravimetrically. [c] Determined on conventional SEC equipment (35 °C) as polystyrene relative values. [d] Overall intrinsic viscosity determined by on-line viscometry. [e] Absolute molecular weight determined by on-line MALLS. [f] Sample not used in averaging of light scattering and viscometry profiles (M_{LS} vs. t_{el}, $[\eta]$ vs. t_{el}).

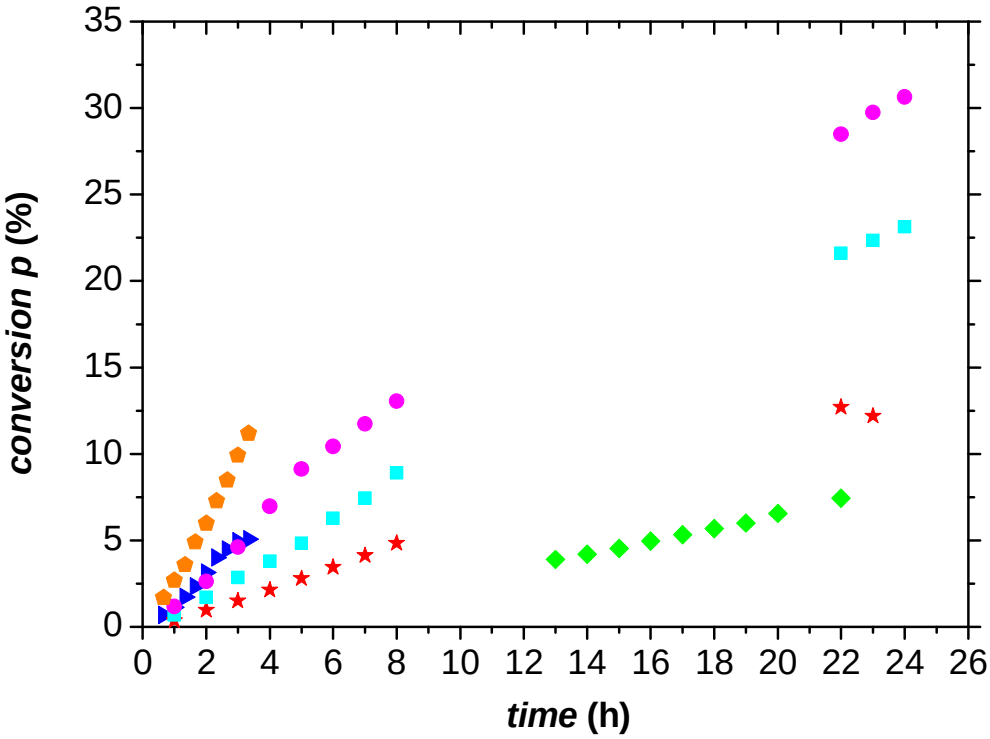

Figure S1. Evolution of conversion with reaction time for conventionally controlled free radical polymerizations with different initial initiator concentrations $[Ini]_0$: 1.0 mM (green, polymerization run A), 2.5 mM (red, run B), 4.5 mM (cyan, run C), 8.5 mM (magenta, run D), 17.1 mM (blue run E), 34.1 (orange, run F). All other reaction conditions are provided in Table 1 of the main manuscript.

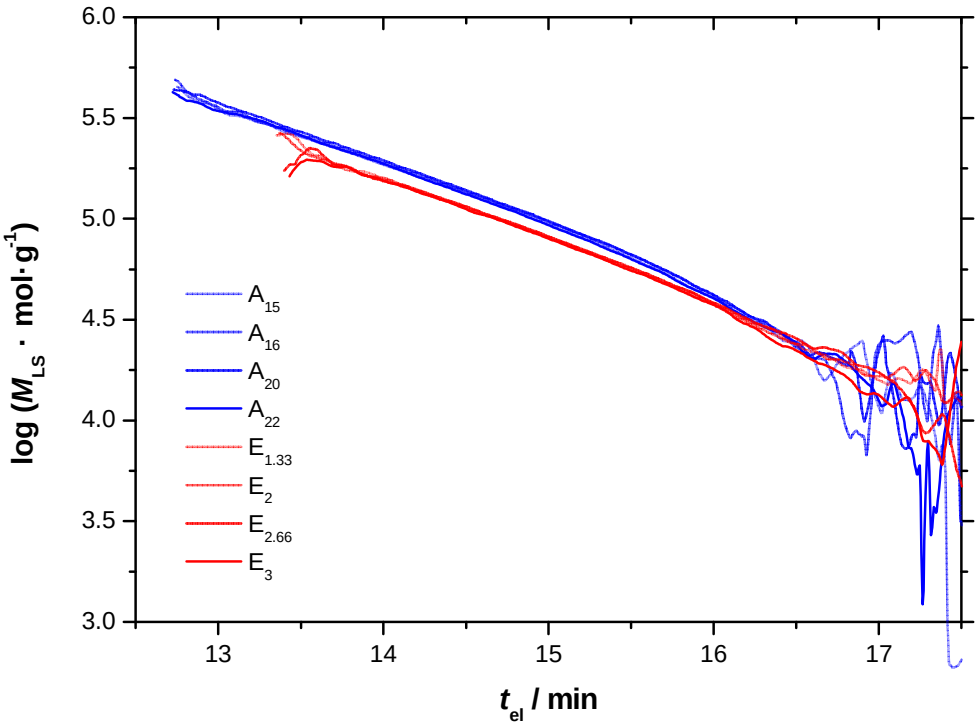

Figure S2. Logarithmic plot of the weight average molecular weight as a function of retention time for polymerizations with two different initial initiator concentrations as obtained from on-line MALLS: Run A with a concentration of 1.0 mM (blue lines) and run E with a concentration of 17.1 mM (red lines). Each line represents the evolution of M_{LS} for a sample taken at a different polymerization time. Curves are given in the order of increasing conversion as visualized by a deepening in color. The data provided are an average over three consecutive sample injections.

Procedure for the Evaluation of On-Line Light Scattering and Viscometry Data

Evaluation of triple SEC data was performed as described in the following. On-line viscometry and MALLS data were averaged over three consecutive injections prior to further processing. In contrast to several other studies of local dispersity indices, no raw data fitting was performed to avoid the interpretation of smooth but inaccurate data. While $M_{LS}(t_{el})$ was directly obtained from on-line light scattering, transformation of $[\eta]$ into $M_v(t_{el})$ via the universal calibration principle was required. Therefore, a universal calibration curve was established with narrowly dispersed polystyrene samples and $\log(M_v(t_{el}))$ of NBR was obtained by subtraction of $\log[\eta]$ from the $\log([\eta]_{PS} \cdot M_{PS})$ at each individual elution time, with $[\eta]_{PS}$ and M_{PS} being intrinsic viscosity and weight average molecular weight of the polystyrene samples, respectively. Each of the described steps of data processing is documented for sample B_{22} in Fig. S3-S6.

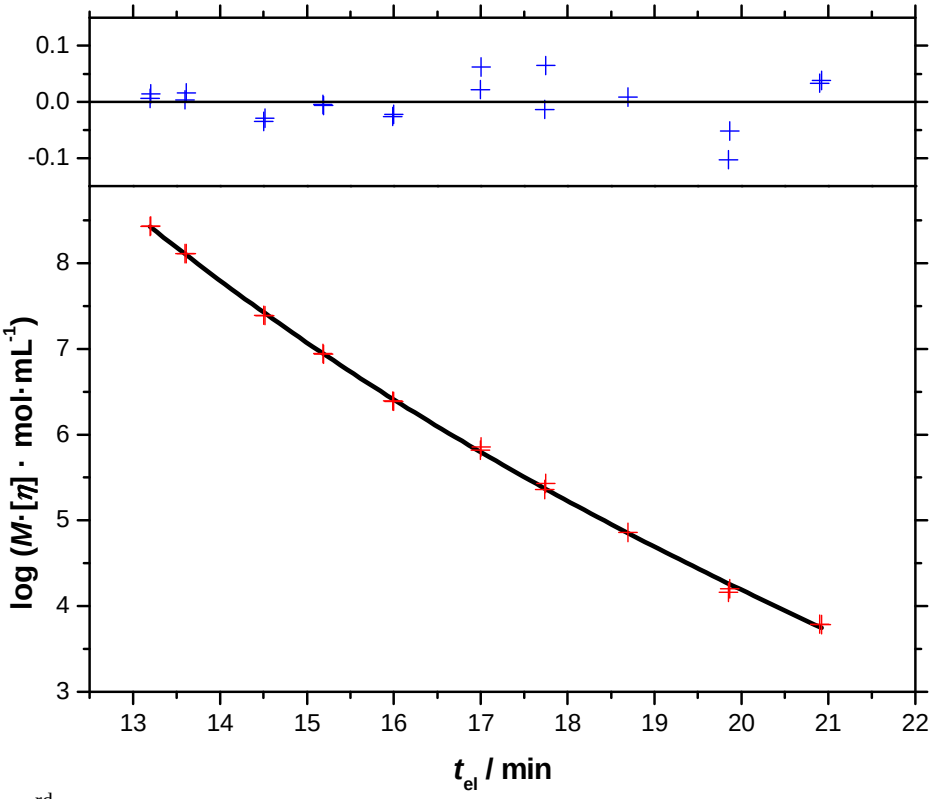

Figure S3. 3rd order polynominal fit (black solid line) of the universal calibration data (red) as a function of retention time. Intrinsic viscosity was determined by on-line viscometry; molar masses were used as provided by the supplier. A regular residual analysis is depicted in the upper panel (blue data points). An excellent fit with an r^2 value of 0.999 is obtained.

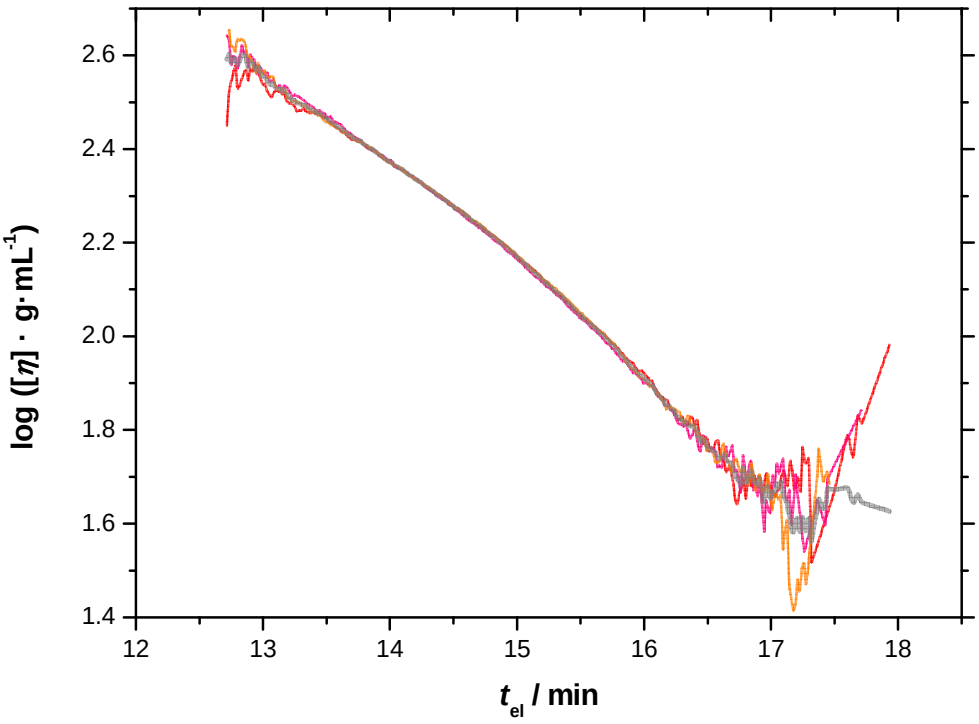

Figure S4. Evolution of intrinsic viscosity, log ($[\eta]$·g·mL^{-1}), with elution time t_{el} measured on-line exemplarily depicted for sample B_{22}. The curves of three consecutive injections (red, orange and pink lines) are averaged (grey line) using the Origin Software to obtain an improved signal-to-noise ratio.

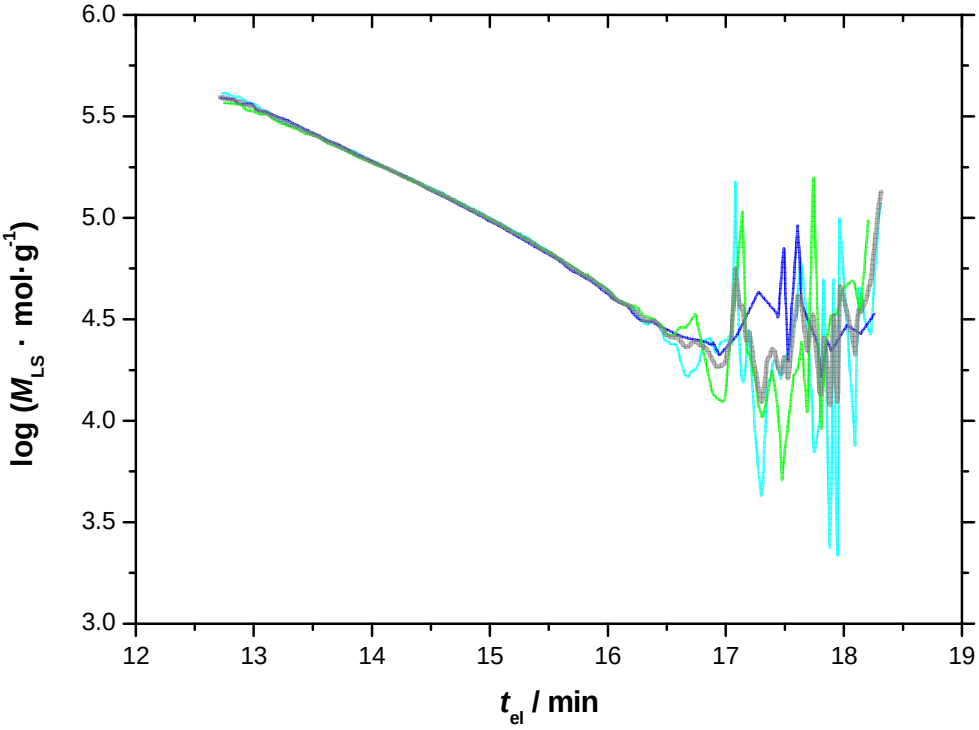

Figure S5. Evolution of weight average molecular weight, log (M_{LS}·mol·g^{-1}), versus elution time t_{el} of sample B_{22} measured via on-line light scattering. The curves of three consecutive injections (blue, green and cyan lines) are averaged (grey line) using the Origin Software to obtain an improved signal-to-noise ratio.

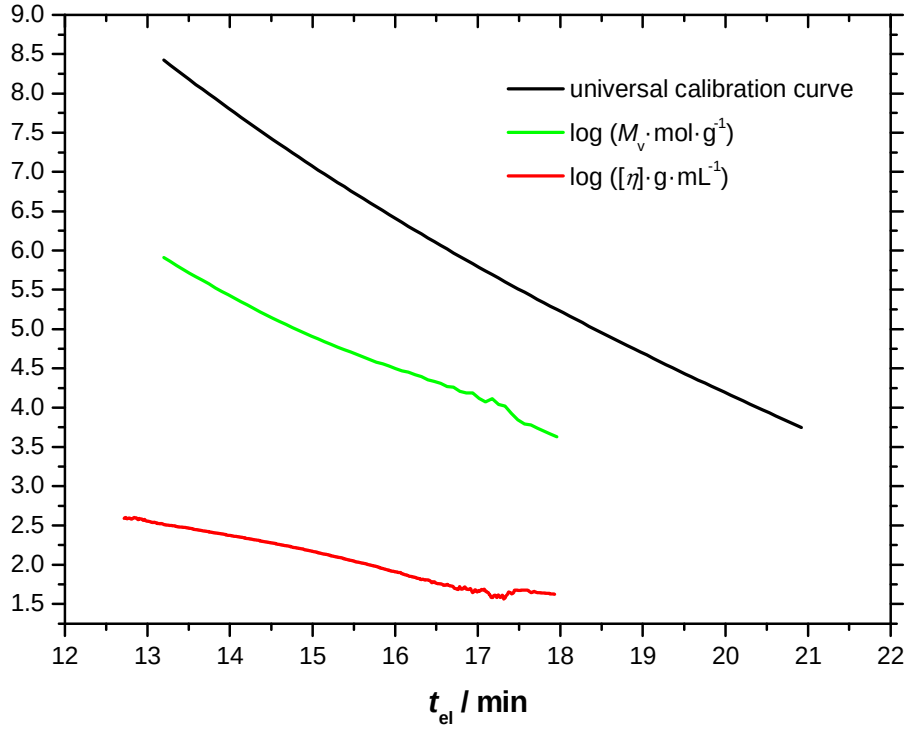

Figure S6. Determination of log (M_v·mol·g^{-1}) of sample B_{22} (green line) as a function of t_{el} from its viscosity profile (red line), log ([η]·g·mL^{-1}), by universal calibration. Log (M_v·mol·g^{-1}) is obtained by subtracting log ([η]·g·mL^{-1}) from the universal calibration curve established for narrowly dispersed polystyrene samples (black line).

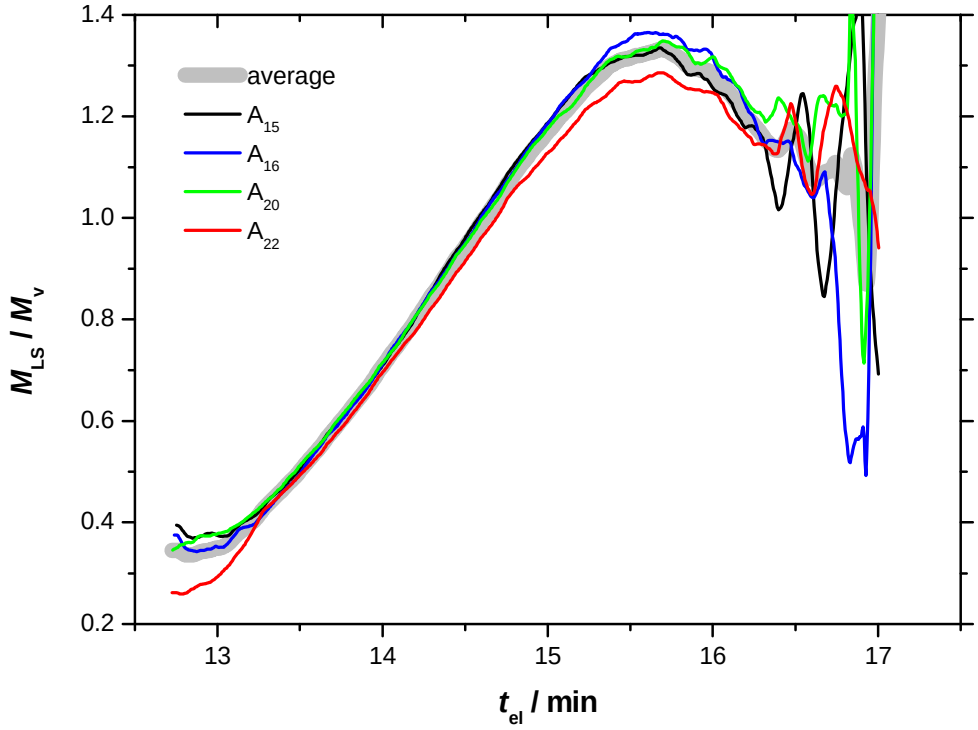

Figure S7. Plot of the local dispersity $Đ(t_{el})$ calculated from on-line MALLS and on-line viscometry SEC. The lines represent the data obtained for samples taken at different polymerization times during polymerization run A ($[Ini]_0$ = 1 mM): A_{15} (black line), A_{16} (blue line), A_{20} (green line) and A_{22} (red line). The curve obtained from averaging over all samples is represented as a grey bold line.

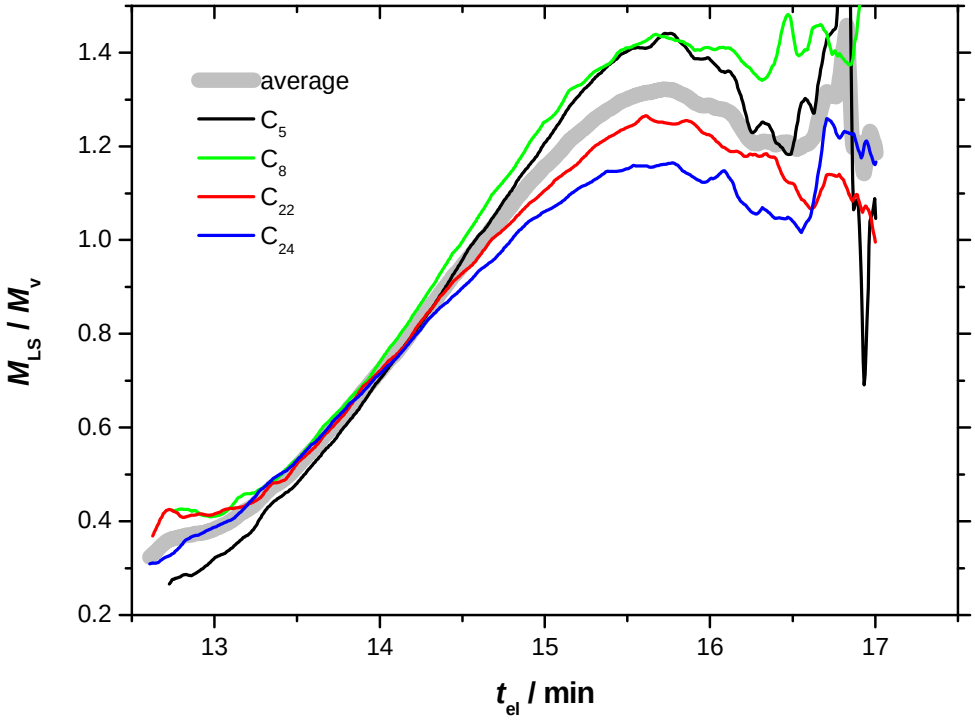

Figure S8. Plot of the local dispersity $Đ(t_{el})$ calculated from on-line MALLS and on-line viscometry SEC. The lines represent the data obtained for samples taken at different polymerization times during polymerization run C ($[Ini]_0$ = 4.5 mM): C_5 (black line), C_8 (green line), C_{22} (red line) and C_{24} (blue line). The curve obtained from averaging over all samples is represented as a grey bold line.

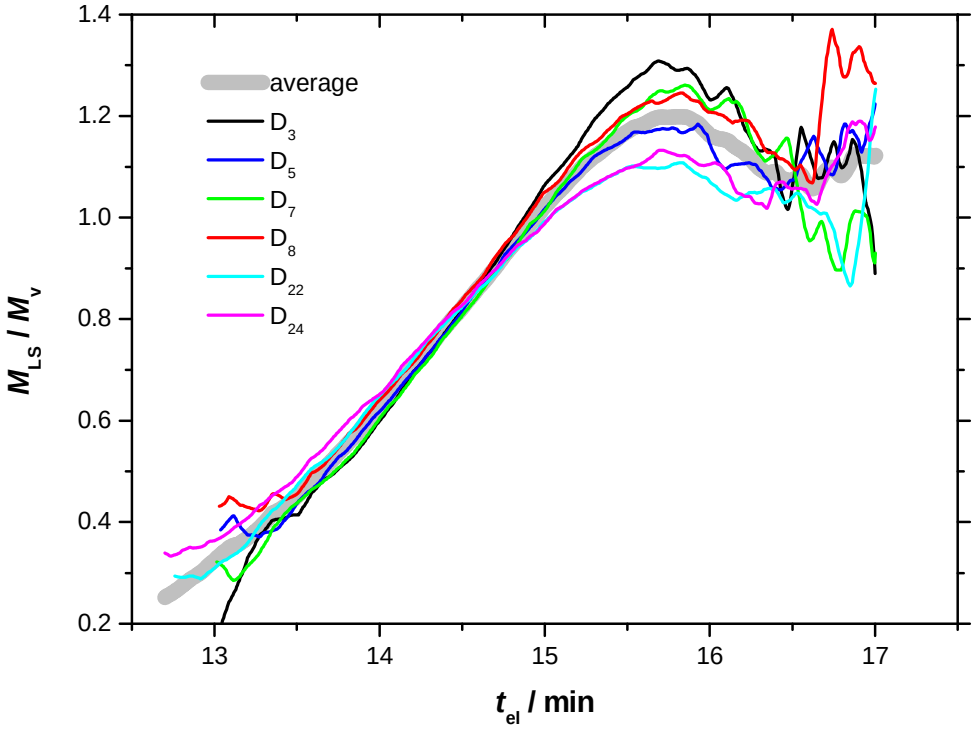

Figure S9. Plot of the local dispersity $Đ(t_{el})$ calculated from on-line MALLS and on-line viscometry SEC. The lines represent the data obtained for samples taken at different polymerization times during polymerization run D ($[Ini]_0$ = 8.5 mM): D_3 (black line), D_5 (blue line), D_7 (green line), D_8 (red line), D_{22} (cyan line) and D_{24} (magenta line). The curve obtained from averaging over all samples is represented as a grey bold line.

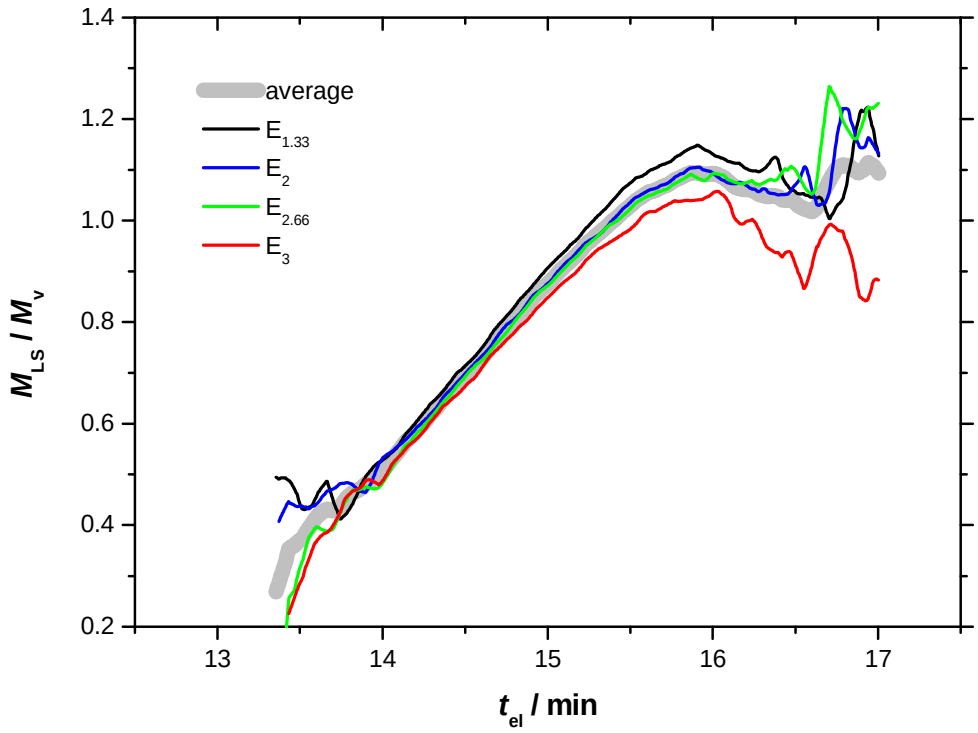

Figure S10. Plot of the local dispersity $Đ(t_{el})$ calculated from on-line MALLS and on-line viscometry SEC. The lines represent the data obtained for samples taken at different polymerization times during polymerization run E ($[Ini]_0$ = 17.1 mM): $E_{1.33}$ (black line), E_2 (blue line), $E_{2.66}$ (green line) and E_3 (red line). The curve obtained from averaging over all samples is represented as a grey bold line.

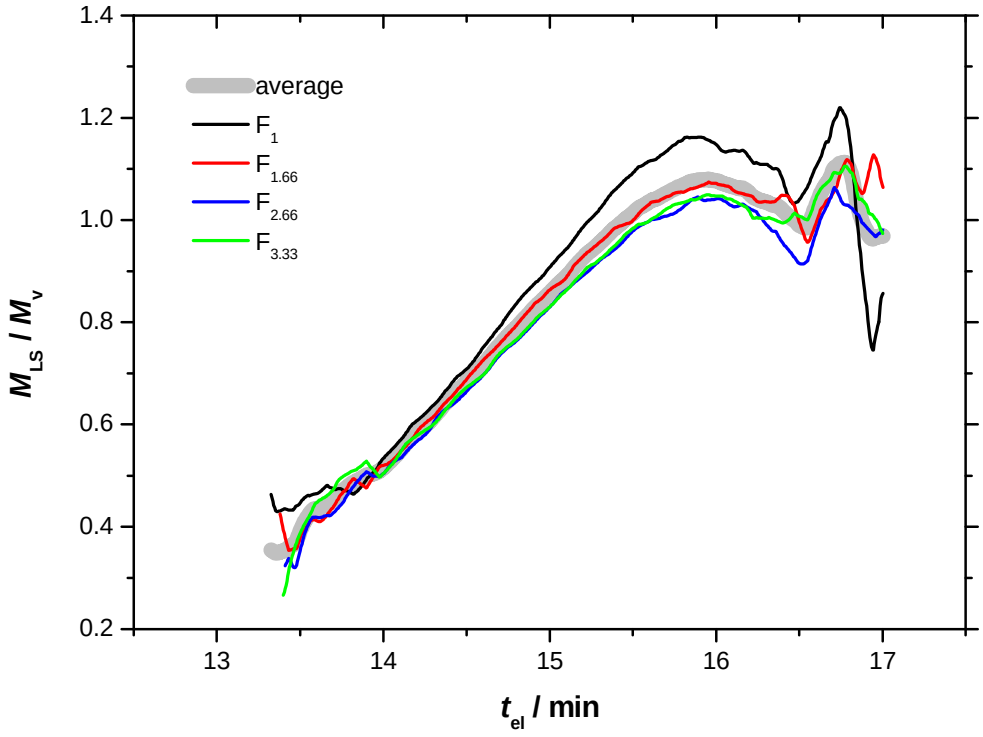

Figure S11. Plot of the local dispersity $Đ(t_{el})$ calculated from on-line MALLS and on-line viscometry SEC. The lines represent the data obtained for samples taken at different polymerization times during polymerization run F ($[Ini]_0$ = 34.1 mM): F_1 (black line), $F_{1.66}$ (red line), $F_{2.66}$ (blue line) and $F_{3.33}$ (green line). The curve obtained from averaging over all samples is represented as a grey bold line.

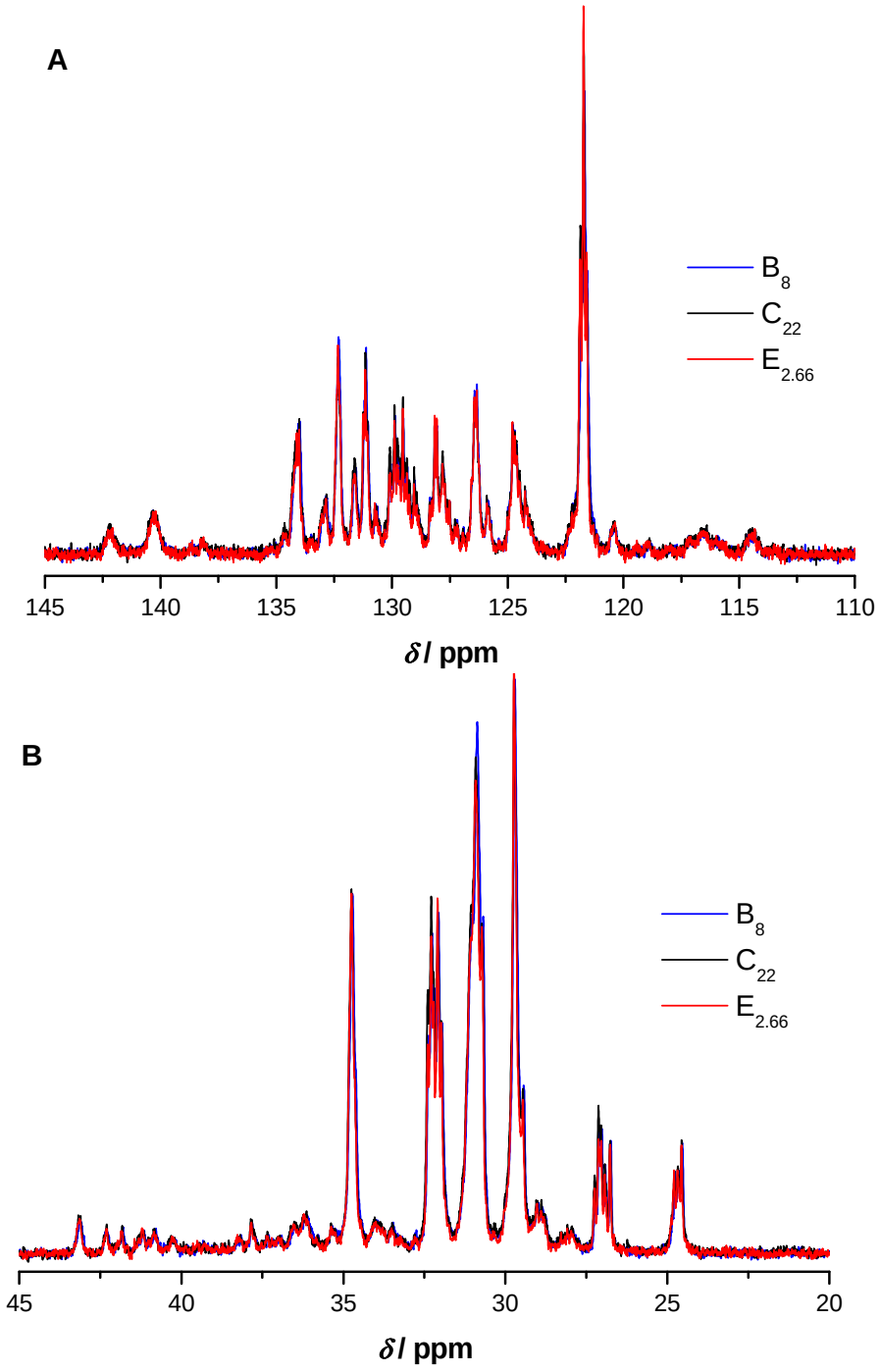

Figure S12. Magnified view into the region of A) 145 to 110 ppm and B) 45 to 20 ppm of the superimposed ^{13}C NMR spectra (ambient temperature, $C_2D_2Cl_4$) of nitrile rubbers B_8, C_{22} and $E_{2.66}$ obtained in conventionally controlled free radical copolymerization of AN and BD. ^{13}C NMR signal assignments of NBR are described in detail elsewhere.[1,2]

Discussion of the Local Dispersity Plots of Samples Taken during RAFT Mediated Polymerization Run G

As depicted in Fig. S13, at a given t_{el}, samples obtained at higher polymerization times exhibit higher values for $Đ(t_{el})$. Nevertheless, at polymerization times of up to 22 h, nitrile rubber of rather uniform microstructure is obtained. $Đ(t_{el})$ span over a shorter range than in the case of conventional free radical copolymerization under equivalent conditions, with $Đ(t_{el})$ provided exemplarily for sample A_{22} (red dotted line). The higher uniformity of the microstructure of polymers obtained in polymerization run G relative to those obtained in polymerization run H can be attributed to both a lower overall radical concentration and a higher concentration of transfer agent relative to radical concentration.

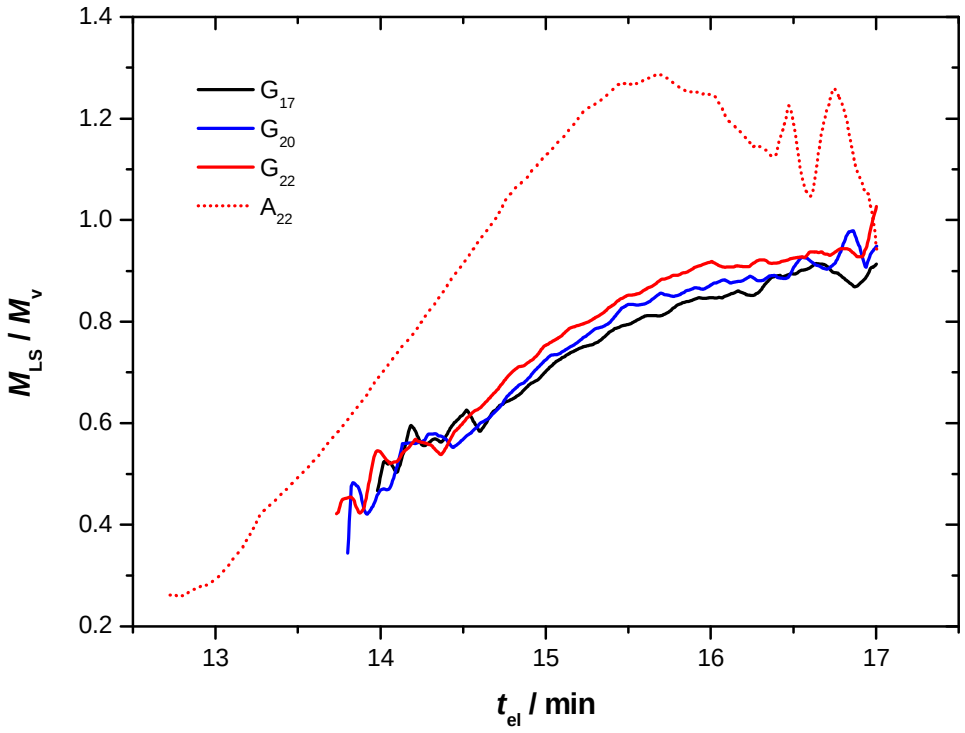

Figure S13. Graphical illustration of the change in polymer microstructure during the RAFT mediated copolymerization of AN and BD with an initial initiator concentration of 1.0 mM (polymerization run G). $Đ(t_{el})$ is depicted for samples G_{17} (black solid line), G_{20} (blue solid line), G_{22} (red solid line) and A_{22} (red dotted line). The latter was obtained from conventionally controlled free radical copolymerization under conditions identical to those applied in RAFT mediated copolymerization G.

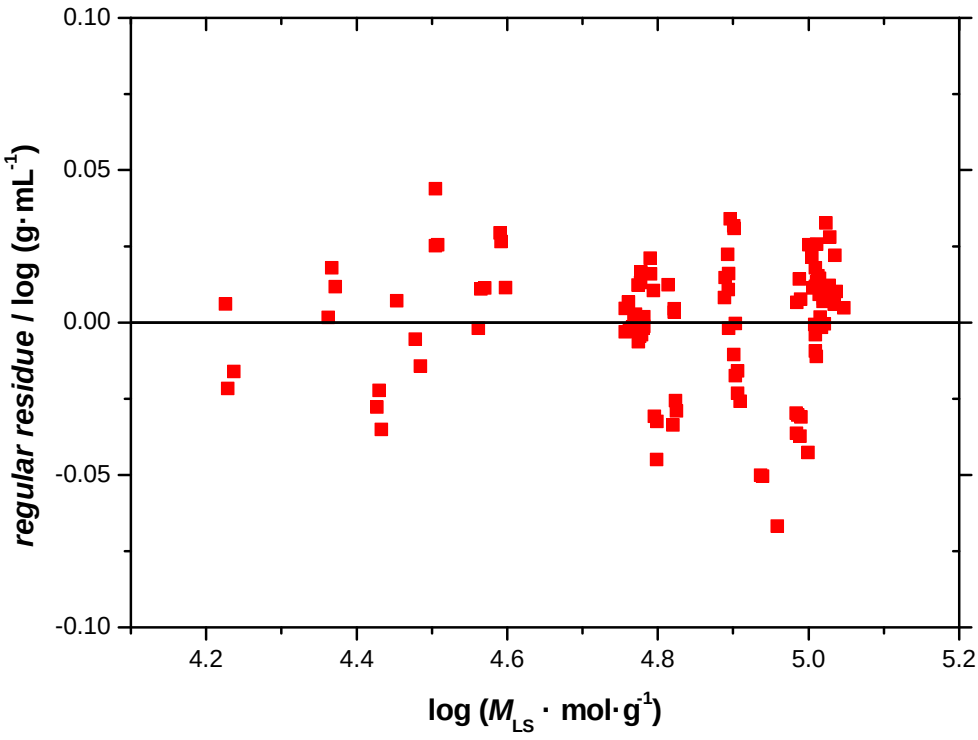

Figure S14. Regular residue of the linear regression applied for the determination of MHKS parameters of NBR (r^2 = 0.979).

Equation S1. Theoretically expected number average molar masses of nitrile rubber (azeotropic conditions) obtained in RAFT mediated copolymerizations G and H. The equation input values of conversion *p*, reaction time *t*, the initial concentration of RAFT agent $[RAFT]_0$ and the initial initiator concentration $[Ini]_0$ are provided in Table S2. The overall monomer concentration $[M]_0$ is 6.75 mM, the molar mass m_{RAFT} of the RAFT agent is 350.6 g·mol^{-1} and the average molar mass m_M of a monomer unit is calculated to 53.7 g·mol^{-1} by the copolymer composition and the molar masses of AN and BD. An initiator efficiency *f* of 0.7 and a value of $d = 1$ for the number of chains produced from radical-radical termination was assumed. A half life $\tau_{1/2}$ (100 °C) of 20 h was deduced from a ten hour half-life decomposition temperature of 110 °C.

$$\overline{M}_n(calc.) = \frac{[M]_0 \cdot p}{[RAFT]_0 + df[Ini]_0(1-\exp(-\frac{\ln 2}{\tau_{1/2}} \cdot t))} m_M + m_{RAFT} \quad \text{(S1)}$$

Table S2. Experimental data and reaction conditions employed in the calculation of the theoretical molar masses of the RAFT mediated copolymerizations G and H via Equation S1.

polymerization run	*t* (h)	p^a (%)	$[Ini]_0$ (mM)	$[RAFT]_0$ (mM)
G	13	1.1	1.0	0.3
G	15	1.5	1.0	0.3
G	17	1.9	1.0	0.3
G	19	2.3	1.0	0.3
G	20	2.6	1.0	0.3
G	22	3.2	1.0	0.3
H	2	1.9	8.5	1.3
H	4	4.5	8.5	1.3
H	6	6.8	8.5	1.3
H	7	8.7	8.5	1.3
H	8	10.5	8.5	1.3
H	22	28.7	8.5	1.3
H	24	29.3	8.5	1.3

[a] Conversion was determined gravimetrically.

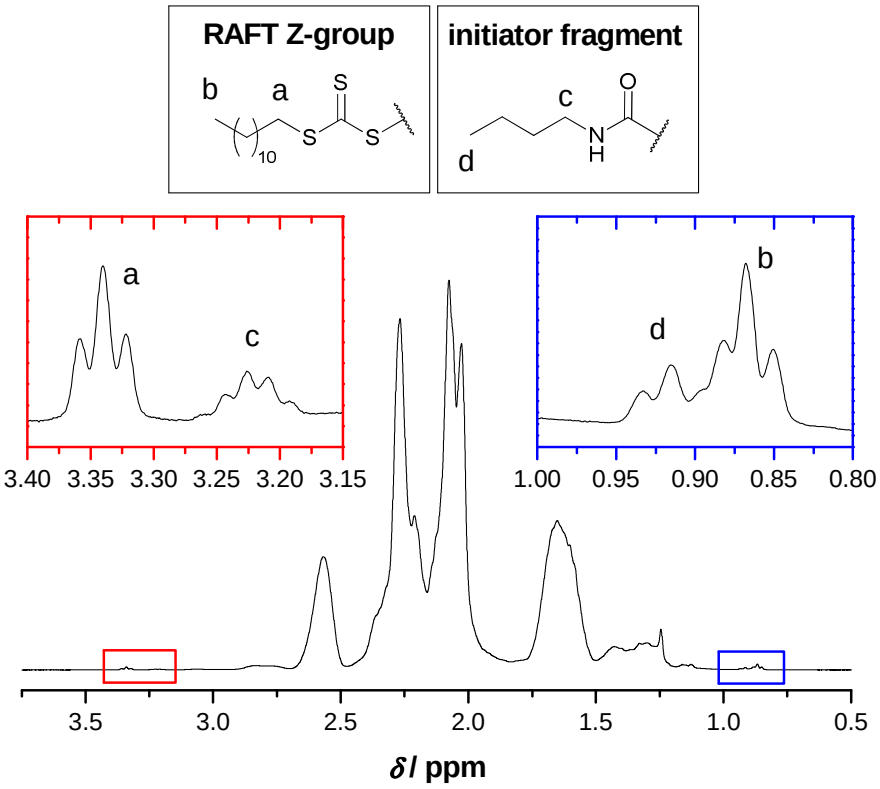

Figure S15. Aliphatic region of the ^{1}H NMR spectrum (ambient temperature, $CDCl_3$) of sample G_{22} obtained in the RAFT mediated copolymerization of AN and BD, evidencing the presence of RAFT polymers and initiator derived chains.

Table S3. Number average molecular weight M_n of NBR samples of polymerizations G and H obtained from apparent calibration and universal calibration using the MHKS parameters determined herein. For practical reasons, in the current work several NBR samples were investigated on a conventional SEC setup with RI detection only (PL-GPC 50 Plus, Polymer Laboratories, see experimental section in the main manuscript).

sample	apparent calibration[a] M_n triple SEC setup (kg·mol^{-1})	apparent calibration[b] M_n conv. setup (kg·mol^{-1})	universal calibration[c] M_n triple SEC setup (kg·mol^{-1})	universal calibration[d] M_n conv. setup (kg·mol^{-1})
G_{17}	44	40	24	20
G_{20}	48	44	26	22
G_{22}	50	46	27	24
H_4	24	24	13	12
H_6	35	33	19	17
H_7	37	36	20	18
H_8	41	40	22	21
H_{22}	69	65	38	33
H_{24}	72	73	39	37

[a] Polystyrene equivalent values obtained via SEC on the triple SEC setup by using the RI detector signal and polystyrene calibration. [b] Polystyrene equivalent values obtained via SEC on conventional SEC equipment. [c] Obtained via universal calibration SEC on the triple SEC setup employing the RI detector signal and the MHKS parameters determined in the current study. [d] Obtained via universal calibration SEC on conventional SEC equipment employing the MHKS parameters determined in the current study.

Re-Evaluation of Polymer-Polymer Coupling SEC Data Employing the Novel MHKS Parameters of NBR

In our previous studies, alkyne-functionalized nitrile rubber (NBR^{func}) has been the subject of orthogonal conjugation upon addition of small molecule diazide linkers to obtain high molecular weight NBR-*b*-NBR by a concept depicted in Scheme S1.[3] Quantitative conversion of chain-end functionality has been confirmed via NMR and mass spectrometry measurements. Since no MHKS parameters of NBR were accessible at the time, merely qualitative information evidencing the conjugation were obtained from SEC showing shifts of the peak retention times. The SEC data were thus re-evaluated with the MHKS parameters obtained in the current study. Molar masses $M_{n,univ}$ of NBR^{func} obtained from universal calibration with the MHKS parameters are provided in Table S4, giving values between 0.5 and 35 kg·mol^{-1}. As coupling of polymers showing molecular weight distributions is a convolution process and molar mass is considered as a quantitative measure in modular conjugations,[4,5] a doubling of M_n is expected during polymer-polymer conjugation. In Table S4, the molar masses $M_{n,app}$ and $M_{n,univ}$ of the coupled polymers NBR-*b*-NBR determined via apparent (*i.e.* relative to polystyrene) and universal calibration, respectively, are compared to the theoretically expected values $M_{n,exp}$. The theoretically expected molar masses are calculated by doubling the molar masses $M_{n,univ}$ of the chain-end functional precursors NBR^{func} under the assumption of a full preservation of the chain-end functionality during the polymerization and a full conversion during the coupling process. The molar masses $M_{n,app}$ obtained in apparent calibration give molar masses of the coupled polymers ranging from 2.5 to 97 kg·mol^{-1}, thus a deviation (δ_{app}) of 39 to 150% from the expected molar masses is observed. In contrast, the molar masses $M_{n,univ}$ of NBR-*b*-NBR obtained in universal calibration range from 1.2 to 50 kg·mol^{-1} and show a much improved agreement with the theory; deviations

(δ_{univ}) lie between 8 and 29%. Nevertheless, molar masses of NBR-*b*-NBR arrange below the theoretically expected values. Since in the previous study[3] the completeness of orthogonal conjugation reactions was confirmed with independent methods, the improved consistency of molar mass data obtained in universal calibration is a further indication for the quality of the MHKS parameters of nitrile rubber obtained herein.

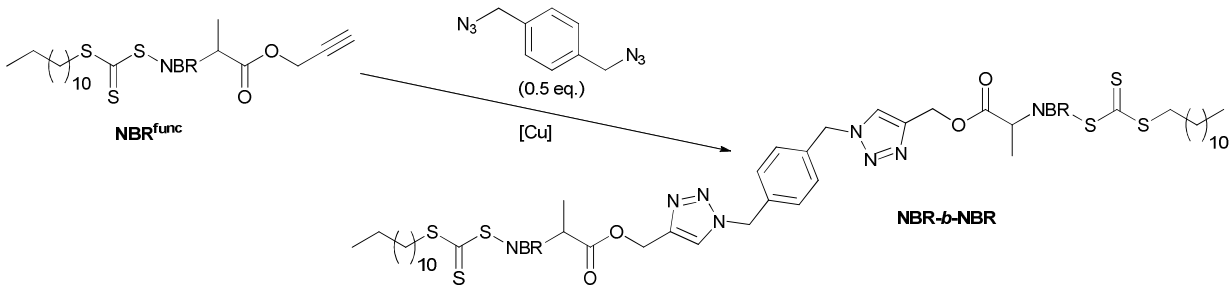

Scheme S1. Concept of orthogonal conjugation of alkyne-functionalized nitrile rubber to obtain high molecular weight NBR via the copper mediated azide-alkyne cycloaddition.

Table S4. Comparison of apparent molecular weight data (relative to polystyrene) versus universal calibration molecular weight data of NBR-NBR conjugation experiments.[a]

entry	NBR[func]	NBR-*b*-NBR				
	universal calibration[b] $M_{n,univ}$ (kg·mol^{-1})	apparent calibration[c] $M_{n,app}$ (kg·mol^{-1})	δ_{app}[d] (%)	$M_{n,exp}$[e] expected (kg·mol^{-1})	universal calibration[b] $M_{n,univ}$ (kg·mol^{-1})	δ_{univ}[f] (%)
1	0.5	2.5	150	1.0	1.2	20
2	3.0	10.6	77	6.0	5.2	13
3	5.2	17.4	67	10.4	8.6	17
4	19.9	72	80	40	37	8
5	35	97	39	70	50	29

[a] Experimental data is taken from Ref. 3. [b] Evaluation of SEC data obtained on conventional SEC equipment (35 °C) was performed with the MHKS parameters obtained in the current study. Note that number average molecular weights determined herein in part are located outside the range of number average molecular weights employed in the determination of the MHKS parameters. [c] Reported as polystyrene relative values obtained on conventional SEC equipment (35 °C). A calibration curve was established with narrowly dispersed polystyrene standards. [d] Deviation of the conventional calibration molar mass $M_{n,app}$ from the expected molar mass $M_{n,exp}$, calculated via $\delta_{app} = |M_{n,app}-M_{n,exp}|/M_{n,exp}$. [e] Molar mass expected from the conjugation being a convolution process: $M_{n,exp}$(NBR-*b*-NBR) = 2 × $M_{n,univ}$(NBR^{func}). [f] Deviation of the universal calibration molar mass $M_{n,univ}$ from the expected molar mass $M_{n,exp}$, calculated via $\delta_{univ} = |M_{n,univ}-M_{n,exp}|/M_{n,exp}$.

References

1. A. Kondo, H. Ohtani, Y. Kosugi, S. Tsuge, Y. Kubo, N. Asada, H. Inaki and A. Yoshioka, *Macromolecules*, 1988, **21**, 2918-2924.
2. L. Li, C.-M. Chan and L. T. Weng, *Macromolecules*, 1997, **30**, 3698-3700.
3. C. J. Dürr, S. G. J. Emmerling, P. Lederhose, A. Kaiser, S. Brandau, M. Klimpel and C. Barner-Kowollik, *Polym. Chem.*, 2012, **3**, 1048-1060.
4. C. Barner-Kowollik, *Macromol. Rapid Commun.*, 2009, **30**, 1625-1631.
5. C. M. Preuss and C. Barner-Kowollik, *Macromol. Theory Simul.*, 2011, **20**, 700-708.